Hindawi
Journal of Combustion
Volume 2018, Article ID 5981598, 7 pages
https://doi.org/10.1155/2018/5981598

Research Article

Experimental Investigation of Combustion Kinetics of Wood Powder and Pellet

Peng Haobin,[1] Yuesheng Li,[2] Yunquan Li,[2] Fangyang Yuan,[3] and Guohua Chen[1]

[1]*School of Mechanical and Automotive Engineering, South China University of Technology, Guangzhou 510640, China*
[2]*Guangdong Institute of Special Equipment Inspection and Research Shunde Branch, Shunde 528300, China*
[3]*School of Mechanical Engineering, Jiangnan University, Wuxi 214122, China*

Correspondence should be addressed to Guohua Chen; mmghchen@scut.edu.cn

Received 3 May 2018; Revised 15 July 2018; Accepted 30 July 2018; Published 2 September 2018

Academic Editor: Hiroaki Watanabe

The combustion kinetic characteristics of wood powder and pellet were investigated within thermogravimetric analyser (TGA) and tube furnace system. The kinetic parameters of these two different forms of woody fuel were measured and derived by double-step-and-double-equal and isothermal method, respectively. The results showed that the combustion mechanisms of wood powder kept consistent through the whole process, while the combustion mechanisms of wood pellet differed significantly between the volatile and char combustion stages. The most probable mechanism functions of the two different forms of woody fuel were not the same due to the differences in internal heat and mass transfer properties. In addition, activation energy values varied from 92.33 kJ·mol^{-1} for wood powder to 71.20 kJ·mol^{-1} for wood pellet, while the preexponential factor value of wood powder (2.55×10^{8} s^{-1}) was far greater than the one of the wood pellet (78.55 s^{-1}) by seven orders of magnitude.

1. Introduction

Suffering the consequences of excessive use of fossil fuel, the countries all over the world contribute more and more to renewable energy development and utilization [1–3]. Biomass energy is the most potential renewable energy in near future, because it is easy to store and convenient to transport and its application technology is ordinary and mature. Furthermore, from production to utilization, the cycle chain of CO_2 emissions from biomass fuel closes to zero [4, 5]. The annual use of wood, widely in construction, furniture manufacturing, packaging, and handicraft, is more than 400 million m^3, yet the processing rate is only about 65% [6]. The remaining compounds such as leftover sawdust should be utilized vigorously to promote energy conservation and emission reduction [7, 8]. The most effective way to use the remains is to extrude them into granules with uniform shape and density and then directly burn them for heating and power generation [9–11].

The previous researches of biomass granular fuel mainly focus on the macro combustion characteristics. Ge et al. [12] calculated the comprehensive combustion characteristics of four kinds of the man-made board in air atmosphere by the thermogravimetric curve and compared the characteristics of synthetic combustion performances. Cuiping et al. [13] piecewise compared the combustion characteristics of three types of granular fuels, namely, corn straw, wood sawdust, and mixed sawdust, through the apparent activation energy values and the preexponential factor values under different combustion stages. Qing et al. [14] calculated the activation energy values and the preexponential factor values of four kinds of biomass materials by the Coats-Redfern method and the first order model, and they came to a conclusion that the wood sawdust is less active than the remaining three species of herbaceous biomass. The calculation compared well with the experimental results. In addition, some scholars explored the granular fuel pyrolysis and combustion rules by mathematical simulation, such as Haseli [15], establishing a mathematical model to describe the combustion process of a single biomass particle, based on a one-dimensional model of quality, momentum, and energy conservation during combustion, with the combination of combustion, pyrolysis kinetic equations.

Table 1: Proximate and ultimate analysis of biomass granular fuel.

Proximate analysis /wt %				Ultimate analysis /wt %				
M_{ad}	V_{ad}	A_{ad}	FC_{ad}	$[C]_{daf}$	$[H]_{daf}$	$[O]_{daf}$	$[N]_{daf}$	$[S]_{daf}$
5.55	83.08	1.32	10.05	52.02	5.07	42.46	0.41	0.04

Owing to the advantages of quick transmission of mass and heat and to acquire more accurate kinetic features of the experimental materials, the samples in kinetic experiments were mostly in fine particles (diameter <0.20 mm) and in small amount (<20 mg) [16–20]. However, the internal heat and mass transfer should not be ignored because of the objective existence while researching on the combustion kinetics of the whole granule [17, 21]. For the best of our knowledge, there was no combustion kinetic research of wood pellet based on the isothermal method in previous studies. To further explore the differences in the combustion kinetic characteristics between wood powder and pellet, some thermal kinetic analyses were conducted in the respective status of the same kind of wood. The results are expected to be the supplement to the existing research of wood pellet combustion kinetics.

2. Materials and Methods

2.1. Materials. The experimental materials were wood-based granular fuel produced by a contract-energy-management enterprise in Foshan, Guangdong. The sawdust and residues produced during furniture manufacturing were crushed and squeezed into densified cylindrical granules with approximately 8 mm in diameter, 40-60 mm in length, and about 950 kg/m^3 in density, including eucalyptus, fir, beech, and walnut, collectively referred to as miscellaneous wood. The samples could be represented by sampling in dispersive points from the same product batch. According to the national standard DL/T 568 and GB/T 28731, the proximate analysis and ultimate analysis results are listed in Table 1. Before the experiment, some pellets were cut to both ends of the flush, with the mass of 1000 ± 5 mg, and the others were ground and sieved to powders with the diameter less than 0.18 mm. All samples were stored in a desiccator standby.

2.2. Apparatus and Instrument

2.2.1. Wood Powder Analysis. The experiments were conducted in an STA-449F3 thermogravimetric analyser (NETZSCH, Germany), with powder samples weighing approximately 10.0 mg, using air as the atmosphere gas at the flow rate of 60 mL/min. The reaction temperature rose to 1000°C from the environmental temperature in heating rates of 10, 20, 30, and 40°C/min, respectively.

2.2.2. Wood Pellet Analysis. The experiments of wood pellet were conducted in a self-made tube furnace system. The main part of the device was a tube reactor, typed SK-4-4-16Q, with an inner diameter of 60 mm and mid-effective heating length of 300 mm, produced by Wuhan Yahua Electric Furnace Ltd. When the experiment began, the influx of air was fed into the tube furnace at the flow rate of 3 L/min. As the furnace atmosphere was stable and the temperature reached the set value, i.e., 800, 1000, 1200, and 1400°C, a corundum crucible carrying a pellet was put into the center of the reactor rapidly, and then the sample was ignited. Afterwards at the selected time moment, i.e., 12, 24, . . ., 60, 90, . . ., 210 s, the crucible was taken out and put into a vessel filled with argon immediately, and then the vessel was sealed tightly and put into a water sink to cool down quickly. After that, the sample which kept the morphology, composition, and properties was weighed, and finally a set of isothermal TG (Thermal Gravity Analysis) curves were drawn.

2.3. Method. The combustion process of wood obeys the Arrhenius law; the basic kinetic equation is generally described as follows:

$$\frac{d\alpha}{dt} = k(T) f(\alpha) = A \exp\left(-\frac{E}{RT}\right) f(\alpha) \quad (1)$$

where α is the conversion of the combustible part of the sample, which is described as follows:

$$\alpha = \frac{m_0 - m_t}{m_0 - m_\infty} \quad (2)$$

where m is the mass of the sample; m_0, m_t, and m_∞ are, respectively, the mass of the sample at initial time, t moment, and finally time; $k(T)$ is the combustion rate constant; A is preexponential factor, s^{-1}; E is apparent activation energy, kJ/mol; R is the ideal gas law constant, 8.314 J/(mol·K); and $f(\alpha)$ is the reaction model.

2.3.1. Wood Powder Thermogravimetric Analysis. By the double-step-and-double-equal method for wood powder, concrete steps are as follows [22].

(a) Determination of Most Probable Mechanism Function $G(\alpha)$. Equation (3) is integrated and transformed into Flynn-Wall-Ozawa equation as

$$\lg\beta = \lg\left[\frac{AE}{RG(\alpha)}\right] - 2.315 - 0.4567\frac{E}{RT} \quad (3)$$

where β is the heating rate, obtained from the formula as follows:

$$\beta = \frac{dT}{dt} \quad (4)$$

transforming (3) into

$$\lg G(\alpha) = \left(\lg\frac{AE}{R} - 2.315 - 0.4567\frac{E}{RT}\right) - \lg\beta. \quad (5)$$

Table 2: Nine commonly used mechanism functions.

$G(\alpha)$	Expressions
$D_1(\alpha)$	$\alpha^2 = 0.2500\left(\frac{t}{t_{0.5}}\right)$
$D_2(\alpha)$	$(1-\alpha)\ln(1-\alpha)+\alpha = 0.1534\left(\frac{t}{t_{0.5}}\right)$
$D_3(\alpha)$	$\left[1-(1-\alpha)^{1/3}\right]^2 = 0.0426\left(\frac{t}{t_{0.5}}\right)$
$D_4(\alpha)$	$\left(1-\frac{2\alpha}{3}\right)-(1-\alpha)^{2/3} = 0.0367\left(\frac{t}{t_{0.5}}\right)$
$R_2(\alpha)$	$\left[1-(1-\alpha)^{1/2}\right] = 0.2929\left(\frac{t}{t_{0.5}}\right)$
$R_3(\alpha)$	$\left[1-(1-\alpha)^{1/3}\right] = 0.2929\left(\frac{t}{t_{0.5}}\right)$
$F_1(\alpha)$	$\ln(1-\alpha) = 0.6931\left(\frac{t}{t_{0.5}}\right)$
$A_2(\alpha)$	$[-\ln(1-\alpha)]^{1/2} = 0.8326\left(\frac{t}{t_{0.5}}\right)$
$A_3(\alpha)$	$[-\ln(1-\alpha)]^{1/3} = 0.8850\left(\frac{t}{t_{0.5}}\right)$

By substituting the α at the same temperature on the TG curves corresponding to different heating rates and different mechanism function $G(\alpha)$ in (5), a series of correlation coefficients R^2 can be achieved with lg $G(\alpha)$ -lg β linear regression. The R^2 is closer to 1, the corresponding $G(\alpha)$ describes the wood powder combustion process better, and, hence, the closest one is the most probable mechanism function.

(b) Derivation of E and A. According to (3), a plot of lg β-$1/T$ corresponds to a straight line with the same α at different heating rates and the determinate form of $G(\alpha)$, from which the values of E and A can be derived from the slope and intercept, respectively.

2.3.2. Wood Pellet Thermogravimetric Analysis

(a) Determination of Most Probable Mechanism Function $G(\alpha)$. The most probable mechanism function of granular fuel combustion can be deduced from the coordination of the experimental data and the kinetic models, namely, reduced time method [22]. Nine commonly used mechanism functions (Table 2) were tested in this paper. If an experimental curve overlaps a theoretical curve, or the experimental data points almost fall in one theoretical curve by comparing the square of deviance [22], the $G(\alpha)$ corresponding to the theoretical curve is the most probable mechanism function, through

$$G(\alpha) = kt = \frac{G(\alpha)_{\alpha=0.5}}{G(\alpha)_{\alpha=1.0}}\left(\frac{t}{t_{0.5}}\right) \quad (6)$$

where $t_{0.5}$ is the time length while α=0.5; $G(\alpha)_{\alpha=0.5}$ is the $G(\alpha)$ while α=0.5; and $G(\alpha)_{\alpha=1.0}$ is the $G(\alpha)$ while α=1.0.

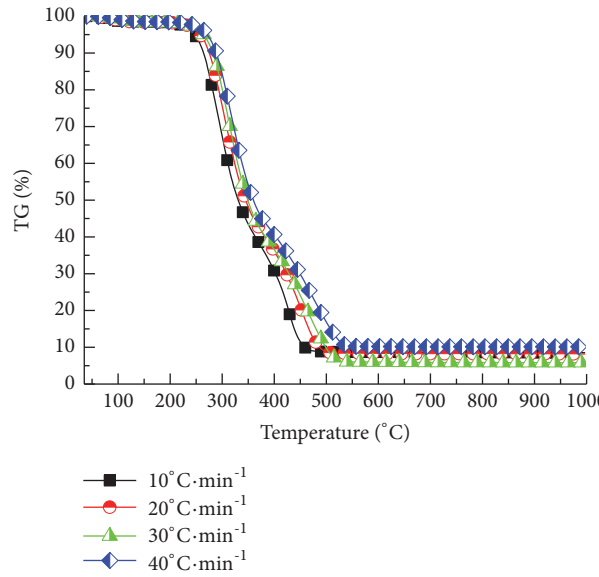

Figure 1: Combustion TG curves of wood powders.

(b) Derivation of E and A. By transforming the determinate most probable mechanism function to plot a straight line including α and t, n and k can be achieved according to the slope and intercept. And then substituting the k_i and T_i corresponding to various temperature sections into Arrhenius equation, one has

$$\ln k = \ln A - \frac{E}{RT}. \quad (7)$$

Plotting the straight line of ln$k$ against $1/T$, E, and A can be derived from the slope and intercept, respectively.

3. Results and Discussion

3.1. The Solution of Combustion Kinetic Parameters of Wood Powder. The TG and DTG (Differential Thermal Gravity) curves of wood powder combustion are shown in Figures 1 and 2, respectively.

By substituting the α at the same temperature in four TG curves, heating rates, and different mechanism functions in (5), with lg$G(\alpha)$-lgβ linear regression, the fitting results were achieved (shown in Table 3). It was clear that the R^2 closest to 1 corresponds to the function $G(\alpha)$=(1-α)^n (n=-1), namely, the most probable mechanism function to describe the combustion process of wood powder.

And then, by substituting the T and β corresponding to the same α at four TG curves of different heating rates and the determinate $G(\alpha)$ in (3), with linear regression of lgβ-$1/T$, a series of E values were derived from the slopes and A values from the intercepts, and the results are shown in Table 4.

The fitting results of E values shown in Table 4 were reliable for the correlation coefficient R^2 values varying from 0.9030 to 0.9991. The results of A values shown in Table 4 were solved according to the E values and the determinate $G(\alpha)$.

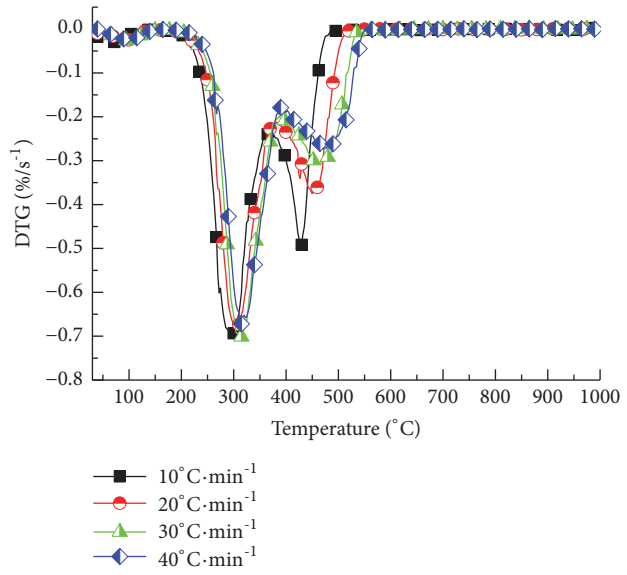

Figure 2: Combustion DTG curves of wood powders.

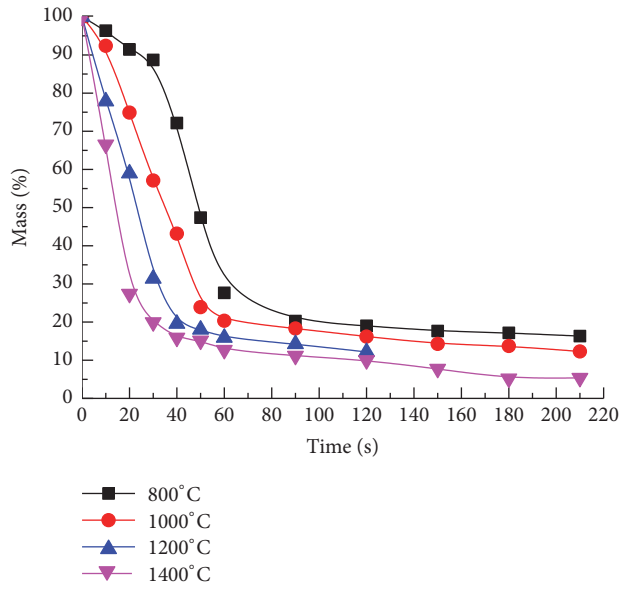

Figure 3: Mass loss curves of wood pellet combustion.

Global average E and A was 92.33 kJ mol^{-1} and 2.55×10^8 s^{-1}, respectively.

3.2. The Solution of Combustion Kinetic Parameters of Wood Pellet

3.2.1. The Determination of Most Probable Mechanism Function $G(\alpha)$. The weight loss curves of wood pellet during isothermal combustion are shown in Figure 3. The fitting results of α-$t/t_{0.5}$ theory and experimental curves are shown in Figure 4. It was clear that the experimental data fell on the theoretical curve of function $G(\alpha)$=$A_2(\alpha)$ or nearby when the conversion rate of α varied in the range of [0.10,0.80).

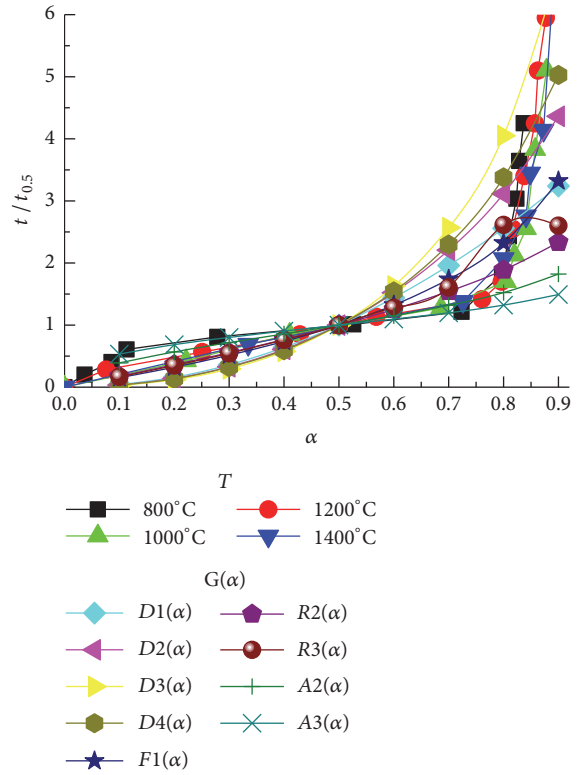

Figure 4: Most probable mechanism function fitting curves of wood pellet combustion reaction.

(a) The Derivation of E and A. The most probable mechanism function $A_2(\alpha)$ was transformed from

$$1 - \alpha = e^{-kt^n} \tag{8}$$

transforming (8) into

$$\ln[-\ln(1-\alpha)] = n\ln t + \ln k. \tag{9}$$

By plotting the straight line of ln[-ln(1-α)]-ln t as shown in Figure 5, the n and k could be derived from the slope and intercept, respectively.

Substitute the k_i and T_i of the four temperature sections into Arrhenius equation as

$$\ln k = \ln A - \frac{E}{RT}. \tag{10}$$

Plotting the straight line of ln$k$ against $1/T$ as shown in Figure 6, E and A were derived from the slope and the intercept to be 71.20 kJ·mol^{-1} and 78.55 s^{-1}, respectively, correlation coefficient R^2 to be 0.9844.

3.2.2. Comparison of Combustion Kinetic Characteristics between Wood Powder and Pellet. Wood pellet combustion is a complex reaction of multiple materials, multiple phases, and multiple steps [15, 24, 25]; thus the kinetics triplet, which might be the apparent result of multistep reactions, usually varies with the combustion condition and the reaction

Table 3: Commonly used mechanism functions [22, 23].

$G(\alpha)$	Mechanism	Expressions	R^2
$G_1(\alpha)$	Power law, n=[1/4 1/3 1/2 3/2 2]	α^n	0.9801
$G_2(\alpha)$	Two-dimensional diffusion	$\alpha + (1-\alpha)\ln(1-\alpha)$	0.9817
$G_3(\alpha)$	Three-dimensional diffusion, n=[1/2, 2]	$\left[1-(1-\alpha)^{1/3}\right]^n$	0.9833
$G_4(\alpha)$	Ginstling-Brounshtein equation	$1-\left(\frac{2}{3}\right)\alpha-(1-\alpha)^{2/3}$	0.9823
$G_5(\alpha)$	Avrami-Erofeev, n=[1/4, 1/3, 2/5, 1/2, 2/3, 3/4, 1, 3/2, 2, 3, 4]	$[-\ln(1-\alpha)]^n$	0.9847
$G_6(\alpha)$	Chemical reaction, $n\neq1$	$\frac{\left[1-(1-\alpha)^{1-n}\right]}{(1-n)}$	0.9934
$G_7(\alpha)$	Phase boundary controlled reaction, n=[1/4, 1/3, 1/2, 2, 3, 4]	$1-(1-\alpha)^n$	0.9837
$G_8(\alpha)$	Chemical reaction, n=[-2, -1, -1/2]	$(1-\alpha)^n$	0.9992
$G_9(\alpha)$	Index law, n=[1, 2]	$\ln\alpha^n$	0.9954
$G_{10}(\alpha)$	Jander equation, n=[1/2, 2]	$\left[1-(1-\alpha)^{1/2}\right]^n$	0.9825
$G_{11}(\alpha)$	Anti-Jander equation	$\left[(1+\alpha)^{1/3}-1\right]^2$	0.9781
$G_{12}(\alpha)$	Zhuravlev equation	$\left[(1-\alpha)^{-1/3}-1\right]^2$	0.9859
$G_{13}(\alpha)$	P-T equation	$\ln\left[\frac{\alpha}{(1-\alpha)}\right]$	0.9984
$G_{14}(\alpha)$	Three-dimensional diffusion	$3\left[1-(1-\alpha)^{1/3}\right]$	0.9833
$G_{15}(\alpha)$	Two-dimensional diffusion	$2\left[1-(1-\alpha)^{1/2}\right]$	0.9825
$G_{16}(\alpha)$	Chemical reaction (second order)	$(1-\alpha)^{-1}-1$	0.9882
$G_{17}(\alpha)$	Nucleation and growth	$[-\ln(1-\alpha)]^{1/n}$	0.9847
$G_{18}(\alpha)$	Power law	$\alpha^{1/n}$	0.9801

Table 4: Combustion kinetic parameters of wood powders under different conversion rates.

α/%	E/kJ·mol^{-1}	A/s^{-1}	R^2	α/%	E/kJ·mol^{-1}	A/s^{-1}	R^2
0.05	72.70	1.26×10^8	0.9991	0.50	101.96	3.87×10^8	0.9646
0.10	80.05	1.99×10^8	0.9977	0.55	104.17	3.07×10^8	0.9316
0.15	76.29	5.91×10^7	0.9795	0.60	94.52	3.85×10^7	0.9030
0.20	87.46	3.10×10^8	0.9979	0.65	97.86	3.12×10^7	0.9243
0.25	91.47	4.38×10^8	0.9973	0.70	99.62	2.41×10^7	0.9432
0.30	94.60	5.33×10^8	0.9960	0.75	96.90	1.31×10^7	0.9583
0.35	97.52	6.23×10^8	0.9951	0.80	90.22	5.32×10^6	0.9700
0.40	99.69	6.32×10^8	0.9912	0.85	82.78	2.30×10^6	0.9725
0.45	101.83	6.06×10^8	0.9845	-	-	-	-

progress. Designed towards precision and automation, the TGA (thermogravimetric analyser) currently is most suitable for thermal measurement on small amounts and small size of the sample. Hence, there is a certain distortion of wood pellet thermal measurement due to the intense internal heat and mass transfer. The comparison between wood powder and pellet combustion kinetic parameters is shown in Table 5.

From Table 5, it is clear that the mechanism functions of wood powder and pellet are different. The discrepancies indicated that sample size, shape, amount, and heating rate could lead to the difference in combustion mechanism of the same kind of fuel [19]. For wood pellet, when α<0.80, the combustion process could be described by the mechanism function $G(\alpha)=[-\ln(1-\alpha)]^{1/2}$, but when $\alpha\geq0.80$, no function that had been selected could fit the corresponding combustion process, whereas for wood powder, there was no piecewise feature; the whole combustion process could be described by the mechanism function $G(\alpha)=(1-\alpha)]^{-1}$. Referring to the proximate analysis result shown in Table 1, $\alpha = 0.80$ was the dividing point where volatile combustion transits to charcoal combustion, illustrating the fact that the complicated heat and mass transfer effects on combustion of the wood pellet were much greater than those on wood powder due to the complexity of internal structure. Therefore, origin pellet should be used as far as possible in the research targeting kinetic parameters determination.

The values of apparent activation energy E, characterizing the molecular activity of wood pellet and powder, were of the same order with the difference 21.13 kJ·mol^{-1}, indicating the consistency of the two forms of materials. As for the characterization of combustible molecule and oxygen molecule collision frequency [26], the preexponential factor A values of the two materials differed greatly, with the latter being seven orders of magnitude higher than the former, showing

Table 5: Kinetic triplets of wood powder and pellet.

Material	A/s^{-1}	$E/kJ \cdot mol^{-1}$	Mechanism function $[G(\alpha)]$
Wood Powder	2.55×10^8	92.33	$(1-\alpha)^{-1}$
Wood pellet	78.55	71.20	$[-\ln(1-\alpha)]^{1/2}$ $(\alpha < 0.80)$

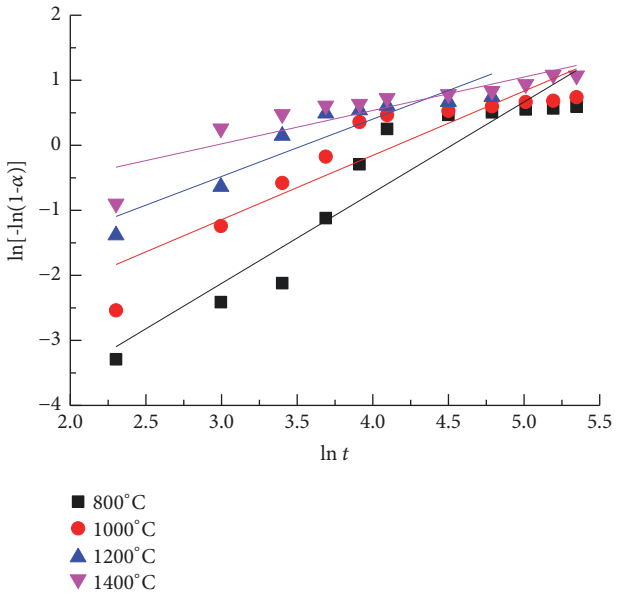

Figure 5: The linear relationship of ln[-ln(1-α)]-ln t.

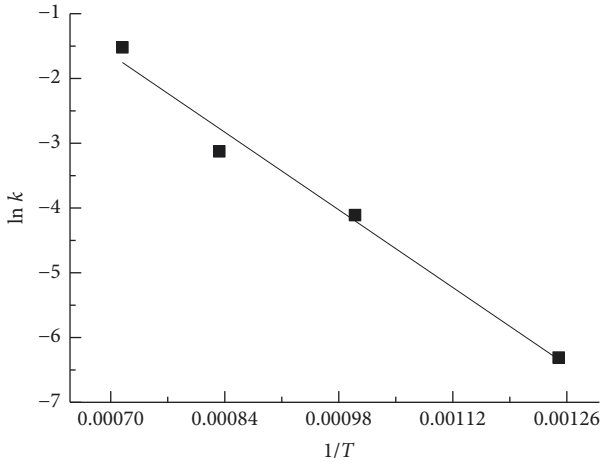

Figure 6: The linear relationship of ln k-1/T.

that the wood powder was much more probable to collide with O_2 than wood pellet in the combustion process. All the calculations were consistent with the apparent phenomenon. In engineering, the former was mainly applied to the layered combustion, and hence good ventilation should be ensured to make the fuel surface fully contacted with the fresh air [27, 28], while the latter was often used in suspension combustion; despite the relatively static state between the fuel and air [29], the fuel still showed good burnout performance for the high molecule collision frequency.

4. Conclusions

By the kinetic analysis and results comparison of the combustion process of wood powder and pellet of the same kind of wood, the following conclusions are drawn:

(1) For wood powder, the combustion mechanism of the whole combustion process was basically unchanged, and the most probable mechanism function had no obvious segmental characteristics; for wood pellet, there was a great discrepancy between volatile combustion stage and char combustion stage, respectively, described by different most probable mechanism functions.

(2) The activation energy E values were 92.33 kJ mol^{-1} for wood powder and 71.20 kJ mol^{-1} for wood pellet, respectively, with a difference less than 30%. The preexponential factor A value of the former (2.55×10^8 s^{-1}) was far greater than that of the latter (78.55 s^{-1}), by seven orders of magnitude.

(3) Currently, most of the TGA is only suitable for combustion kinetic analysis in wood powder with less sample quantity and small particle size; hence it is difficult to truly reveal the combustion kinetic characteristics of bulk granular biomass fuel. In academic researches and engineering applications for the granular fuel, the TGA that is suitable for bulk fuel should be adopted to reduce the experimental errors induced by the sample.

Data Availability

The datasets generated and analysed during this study are available in the FAIRsharing repository: https://figshare.com/s/d51ecef2f1992ae0b7c3.

Conflicts of Interest

The authors declare that there are no conflicts of interest regarding the publication of this paper.

Acknowledgments

The authors thank Shunchun Yao and Saihua Jiang for comments and insights leading to the development of this manuscript. The authors gratefully acknowledge support by South China University of Technology and Guangdong Institute of Special Equipment Inspection and Research, Shunde Branch. This work was supported by Administration of Quality and Technology Supervision of Guangdong Province Research Funds (Grant no. 2017PB08).

References

[1] A. Omri and D. K. Nguyen, "On the determinants of renewable energy consumption: International evidence," *Energy*, vol. 72, pp. 554–560, 2014.

[2] C. Cambero and T. Sowlati, "Assessment and optimization of forest biomass supply chains from economic, social and environmental perspectives – A review of literature," *Renewable & Sustainable Energy Reviews*, vol. 36, pp. 62–73, 2014.

[3] J. Benedek, T. Sebestyén, and B. Bartók, "Evaluation of renewable energy sources in peripheral areas and renewable energy-based rural development," *Renewable & Sustainable Energy Reviews*, vol. 90, pp. 516–535, 2018.

[4] M. Matúš, P. Križan, Ľ. Šooš, and J. Beniak, "The effect of papermaking sludge as an additive to biomass pellets on the final quality of the fuel," *Fuel*, vol. 219, pp. 196–204, 2018.

[5] Z. Liu, B. Fei, Z. Jiang, and X. Liu, "Combustion characteristics of bamboo-biochars," *Bioresource Technology*, vol. 167, pp. 94–99, 2014.

[6] X. Deyan, "Analysis to situation and countermeasure industry of wood manufacture industry of our country," *Forestry Prospect and Design*, vol. no. 3, pp. 85–92, 2013.

[7] F. Guo and Z. Zhong, "Co-combustion of anthracite coal and wood pellets: Thermodynamic analysis, combustion efficiency, pollutant emissions and ash slagging," *Environmental Pollution*, vol. 239, pp. 21–29, 2018.

[8] L. J. R. Nunes, J. C. O. Matias, and J. P. S. Catalão, "Mixed biomass pellets for thermal energy production: A review of combustion models," *Applied Energy*, vol. 127, pp. 135–140, 2014.

[9] S. Proskurina, E. Alakangas, J. Heinimö et al., "A survey analysis of the wood pellet industry in Finland: Future perspectives," *Energy*, vol. 118, pp. 692–704, 2017.

[10] E. Trømborg, T. Ranta, J. Schweinle, B. Solberg, G. Skjevrak, and D. G. Tiffany, "Economic sustainability for wood pellets production - Acomparative study between Finland, Germany, Norway, Sweden and the US," *Biomass and Bioenergy*, vol. 57, pp. 68–77, 2013.

[11] R. Tauro, C. A. García, M. Skutsch, and O. Masera, "The potential for sustainable biomass pellets in Mexico: An analysis of energy potential, logistic costs and market demand," *Renewable & Sustainable Energy Reviews*, vol. 82, pp. 380–389, 2018.

[12] P. Ge, L. Qiang, and X. Peng, "Thermogravimetric study on combustion and kinetic characteristics of artificial-plates," *Techniques and Equipment for Environmental Pollution Control*, vol. 6, pp. 2431–2436, 2012.

[13] W. Cuiping, L. Dingkai, W. Fengyin et al., "Experimental study on the combustion characteristics of biomass pellets," *Transaction of the CSAE*, vol. 22, no. 10, pp. 174–177, 2006.

[14] Q. Wang, W. Zhao, H. Liu, C. Jia, and H. Xu, "Reactivity and kinetic analysis of biomass during combustion," *Energy Procedia*, vol. 17, pp. 869–875, 2012.

[15] Y. Haseli, J. A. van Oijen, and L. P. H. de Goey, "A detailed one-dimensional model of combustion of a woody biomass particle," *Bioresource Technology*, vol. 102, no. 20, pp. 9772–9782, 2011.

[16] X. Fang, L. Jia, and L. Yin, "A weighted average global process model based on two-stage kinetic scheme for biomass combustion," *Biomass & Bioenergy*, vol. 48, pp. 43–50, 2013.

[17] W. Cao, J. Li, and L. Lue, "Study on the ignition behavior and kinetics of combustion of biomass," *Energy Procedia*, vol. 142, pp. 136–141, 2017.

[18] A. I. Moreno, R. Font, and J. A. Conesa, "Combustion of furniture wood waste and solid wood: Kinetic study and evolution of pollutants," *Fuel*, vol. 192, pp. 169–177, 2017.

[19] S. Y. Yorulmaz and A. T. Atimtay, "Investigation of combustion kinetics of treated and untreated waste wood samples with thermogravimetric analysis," *Fuel Processing Technology*, vol. 90, no. 7-8, pp. 939–946, 2009.

[20] P. Jinxing, C. Guanyi, W. Deqin et al., "Kinetic and gaseous product analyses of wood pyrolysis," *Acta Energiae Solaris Sinica*, vol. 32, no. 12, pp. 1719–1724, 2011.

[21] B. Peters and J. Smuła-Ostaszewska, "Simultaneous prediction of potassium chloride and sulphur dioxide emissions during combustion of switchgrass," *Fuel*, vol. 96, pp. 29–42, 2012.

[22] H. Rongzu, *Thermal Analysis Kinetic*, Science Press, Beijing, China, 2008.

[23] R. López-Fonseca, I. Landa, U. Elizundia, M. A. Gutiérrez-Ortiz, and J. R. González-Velasco, "A kinetic study of the combustion of porous synthetic soot," *Chemical Engineering Journal*, vol. 129, no. 1-3, pp. 41–49, 2007.

[24] H. Jiang, M. Bi, B. Li, B. Gan, and W. Gao, "Combustion behaviors and temperature characteristics in pulverized biomass dust explosions," *Journal of Renewable Energy*, vol. 122, pp. 45–54, 2018.

[25] J. Li, M. C. Paul, P. L. Younger, I. Watson, M. Hossain, and S. Welch, "Prediction of high-temperature rapid combustion behaviour of woody biomass particles," *Fuel*, vol. 165, pp. 205–214, 2016.

[26] Q. Wang, Y. Zhao, and Y. Zhang, "Shrinkage kinetics of large-sized briquettes during pyrolysis and its application in tamped coal cakes from large-scale chambers," *Fuel*, vol. 138, pp. 1–14, 2014.

[27] M. Costa, N. Massarotti, V. Indrizzi, B. Rajh, C. Yin, and N. Samec, "Engineering bed models for solid fuel conversion process in grate-fired boilers," *Energy*, vol. 77, pp. 244–253, 2014.

[28] N. Vorobiev, A. Becker, H. Kruggel-Emden, A. Panahi, Y. A. Levendis, and M. Schiemann, "Particle shape and Stefan flow effects on the burning rate of torrefied biomass," *Fuel*, vol. 210, pp. 107–120, 2017.

[29] R. Hurt, J.-K. Sun, and M. Lunden, "A kinetic model of carbon burnout in pulverized coal combustion," *Combustion and Flame*, vol. 113, no. 1-2, pp. 181–197, 1998.